Multi-terminal Conductance of a Floquet Topological Insulator (supplementary material)

L. E. F. Foa Torres,[1] P. M. Perez-Piskunow,[1] C. A. Balseiro,[2,3] and Gonzalo Usaj[2,3]

[1]*Instituto de Física Enrique Gaviola (CONICET) and FaMAF, Universidad Nacional de Córdoba, Argentina*
[2]*Centro Atómico Bariloche and Instituto Balseiro, Comisión Nacional de Energía Atómica, 8400 Bariloche, Argentina*
[3]*Consejo Nacional de Investigaciones Científicas y Técnicas (CONICET), Argentina*

(Dated: October 8, 2014)

In this supplementary material we present further numerical results and details supporting the conclusions of the main text.

Laser-induced gaps in graphene.– The laser-induced gaps in graphene under circular polarization have been studied by many authors since the work by Oka and Aoki [1]. Here we briefly revisit the nature of these gaps.

Let us consider an infinite irradiated ribbon. The Floquet space is the direct product between the usual Hilbert space and the space of time-periodic functions with period $2\pi/\Omega$. This space is spanned by the direct product basis $\{|(k,\pm),n\rangle = |(k,\pm)\rangle \otimes |n\rangle\}$ where $\{|(k,\pm)\rangle\}$ denotes the eigenstates of the graphene Hamiltonian (without radiation) corresponding to wave-vector k bearing a positive/negative projection ($\pm$) on the pseudospin and $\{|n\rangle\}$ is a basis for the space of time-periodic functions, $\langle t|\, n\rangle = \exp(in\Omega t)$. When the laser is switched off, these states are also eigenstates of the full Hamiltonian and the quasi-energy dispersion around one of the Dirac points is as represented in Fig. S1(a) , we have conical dispersions shifted by $\hbar\Omega$. At $\hbar\Omega/2$ one has crossing point between Floquet states corresponding to $n = 0$ and $n = 1$. Turning on the laser introduces a matrix element which lifts the degeneracy between these states, thereby opening a bulk gap (grey lines in the scheme). The eigenstates of the full Hamiltonian acquire therefore a varying weight on the Floquet replicas.

The gap at the Dirac point (see for example Fig. 2(a) of the main text) can be understood in a similar way. The main difference being that the states at the Dirac point (both belonging to $n = 0$, represented in black in Fig.S1(a)) get mixed through a virtual process involving the emission and reabsorption of a photon[1, 2]. In this case, the resulting gap is second order in the electron-photon coupling and the states have almost unit weight on the $n = 0$ replica. One could also note that there are other avoided crossings at zero energy between the replicas with $n = +1$ and $n = -1$, the physics is again similar.

The Floquet Hamiltonian in the radiated and non-radiated areas is represented in Fig. S1(b).

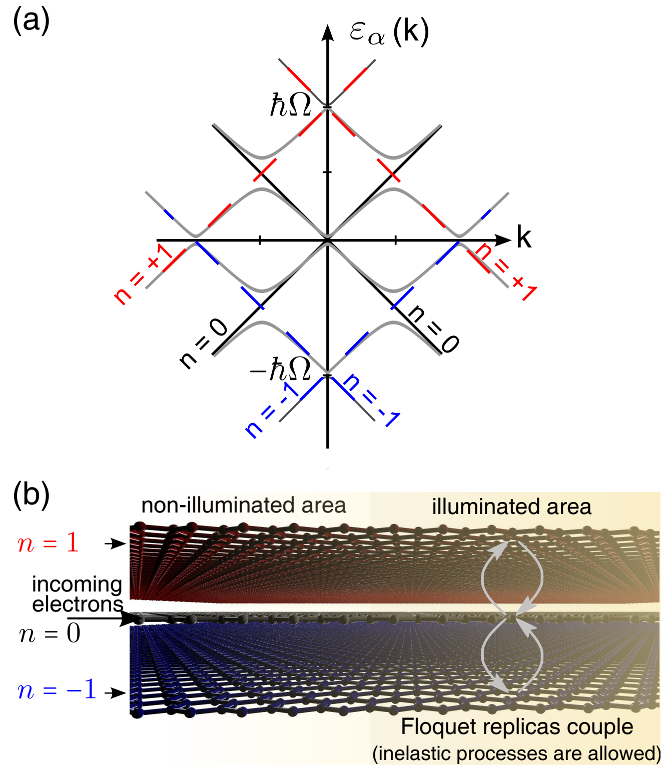

FIG. S1. (a) Scheme of the Floquet quasi-energy dispersion close to the Dirac point in graphene. Floquet replicas are shifted by $\hbar\Omega$, three of them are shown in this plot. When the radiation is switched on the these replicas couple with each other and degeneracies can be lifted (grey lines). This produces gaps around the Dirac point and $\pm\hbar\Omega/2$. (b) Scheme showing the Floquet space using a real space basis for graphene. Far away in the non-illuminated leads the eigenstates correspond to a well-defined index n. Therefore, incoming electrons arrive to the illuminated area from a reference channel ($n = 0$) and may then couple to other replicas through inelastic processes as represented in (b).

Simulation scheme.– The transport simulations were carried out using Floquet scattering theory [3, 4] as outlined in the main text. The transmission probabilities in Eqs. (1-3) as well as the time-averaged density of states can be computed from the Floquet-Green's functions as described in Chapter 6 of Ref. [5].

Simulations with frequencies in the mid-infrared range may offer better chances of experimental realization [6, 7] but would imply a much higher computational cost because a larger system is needed for the chiral edge states to develop at small to moderate laser intensities. The parameters used here are similar to those in the figures of the main text and are chosen for illustration purposes. In the simulations for the hexagonal (rectangular) setup of Fig. 1(c) (Fig. 1b) the laser is turned on in the central part in an area of hexagonal (rectangular) shape and is turned off slowly towards the leads with a decay length of ten lattice constants. This smoothens the interface with the leads.

Pumped current in an H-shaped six terminal configuration.– As mentioned in the text, in a multi-terminal setup inversion symmetry alone does not warrant a zero pumped current. This is specially evident in a graphene sample with the six terminal configuration of Fig. 1(a) of the main text. Figure S2 shows numerical results for the pumped current through each lead in such a setup. We show only the currents in leads 1, 2 and 3 as represented in the scheme. The currents in the remaining leads overlap with those shown: $\bar{\mathcal{I}}_6 = \bar{\mathcal{I}}_1$, $\bar{\mathcal{I}}_2 = \bar{\mathcal{I}}_5$ and $\bar{\mathcal{I}}_3 = \bar{\mathcal{I}}_4$. The inset (a) shows the asymmetry of the corresponding transmission coefficients $\delta\mathcal{T}_j(\varepsilon) = \sum_i(\mathcal{T}_{i,j}(\varepsilon) - \mathcal{T}_{j,i}(\varepsilon))$.

Local density of states at the dynamical gap.– Matching problems between the illuminated sample and non-illuminated leads were shown in the main text to lead to a decrease in the two-terminal conductance following an 'S' shape. As discussed in the main text this reduction/asymmetry of the electronic transmission is not due to the lack of available states. This is clearly shown in Fig. S3 where we present the time-averaged local density of states at two selected energies (a) $E = 0.7\gamma_0$ and (b) $E = 0.8\gamma_0$. In consistency with analytical calculations [6, 7] no appreciable differences between the two panels are observed, the contribution from the chiral edge states in the illuminated part of the sample is clear.

The role of pseudospin on the matching between non-illuminated and illuminated areas.– Now we present some results to support our statement that the pseudospin plays a role on the matching problems found in the numerics for the case of graphene leads without additional doping. Specifically, we computed the projection of the pseudospin along the ribbon direction (where translational invariance holds) in the presence of laser illumination, considering only the $n = 0$ part of the Floquet eigenfunction. The results are shown in Fig. S4, the color scale indicates the value of the pseudospin projection on the corresponding eigenstate. If we sweep the dynamical gap from top to bottom, we can see that pseudospin changes sign when passing from the bottom part of the dynamical gap to the top. Since the pseudospin of electrons incoming from the non-irradiated graphene leads keep their pseudospin projection constant, a mismatch is expected. Transport will then be suppressed on the lower part of the dynamical gap and favoured on the upper part.

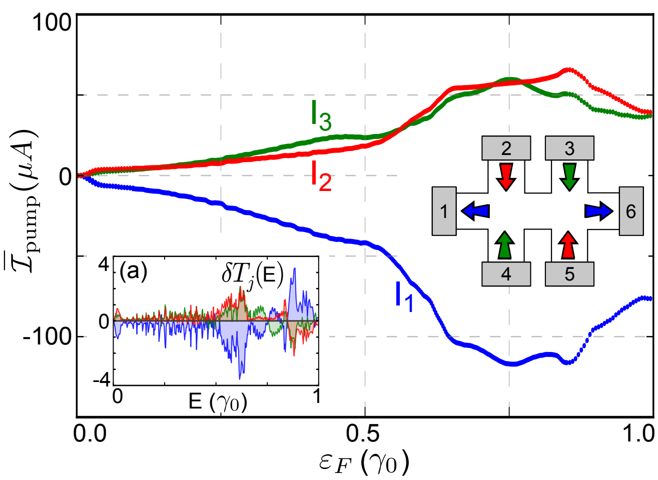

FIG. S2. (main frame) Pumped currents for an H-shaped six terminals configuration as shown in the scheme. Directional asymmetry in the transmission coefficients for terminals 1 to 3 is shown in the inset (a). These results correspond to graphene leads of width $W = 99a$ (1 and 6 are zigzag ribbons, 2-5 are armchair) without additional doping. The radiated area is a square of length $L = 512a$. The laser of frequency $\hbar\Omega = 1.5\gamma_0$ is turned-off slowly over a length of $30a$ and the intensity is parametrized by $z = 0.15$.

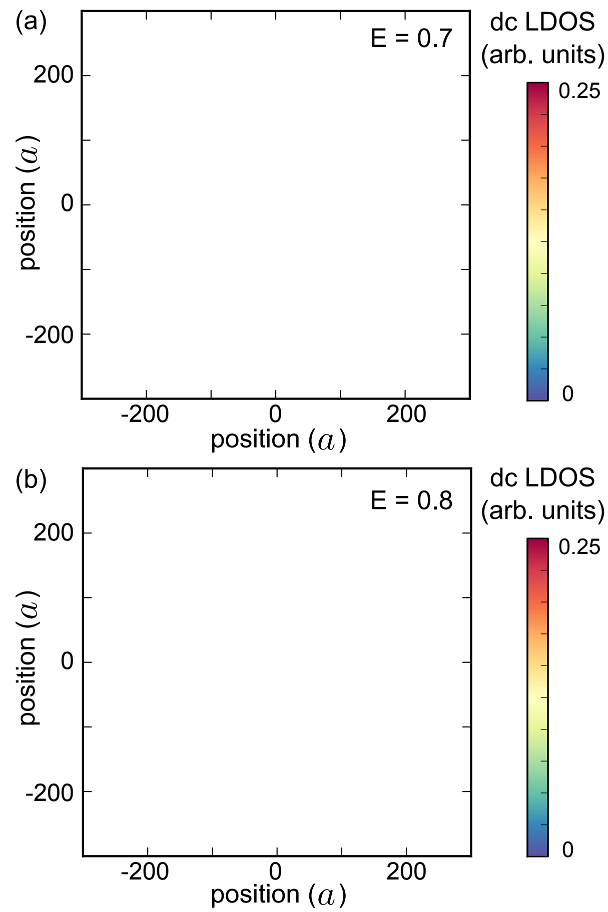

FIG. S3. Time-averaged local density of states for the hexagonal configuration used in Fig. 3 of the main text at two different energies (the same as in Fig. 3(c) and (d)) (a) $E = 0.7\gamma_0$ and (b) $E = 0.8\gamma_0$. While delocalized states are available in the leads, the edge states and the bulk gap are clearly observed within the central part (illuminated area). The parameters are the same as in Fig. 3.

Detail of chiral edge states developing at higher order replicas and with $E \sim 0$.– In the discussion around Fig. 4 we mentioned that only the chiral edge states crossing at $k = \pi/a$ have an important weight on the $n = 0$ channel. In Fig. S5 we show this explicitly. Figs. S5(a) and (b) reproduce Figs. 4(b) and (c) of the main text and show the full Floquet quasi-energy

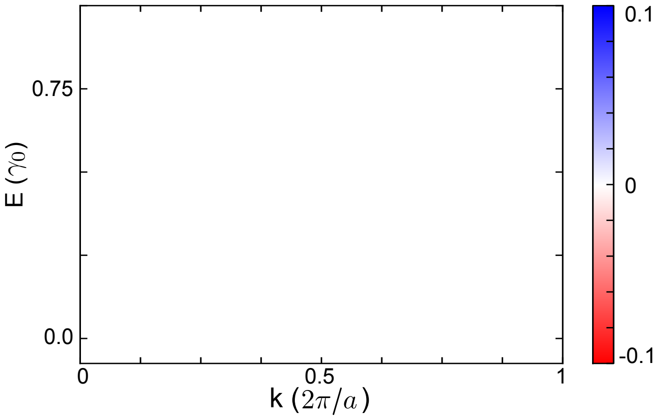

FIG. S4. (a) and (b): Quasi-energy band structure for a zigzag ribbon of width $W = 125a$, in presence of a laser of frequency $\hbar\Omega = 1.5\gamma_0$ and $z = 0.1$. The color scale indicates the expectation value of the pseudospin projected along the ribbon direction and the $n = 0$ Floquet channel. The color scale is saturated above/below 0.1 for better visualization.

structure. Figs. S5(c) and (d) show the same quasi-energy structure in a color scale where the color encodes the weight on the $n = 0$ channel, from zero weight (white) to unit weight (black). The chirality of the edge states away from $k = \pi/a$ is the opposite as those crossing at $k = \pi/a$, this is shown in the inset of Fig. S5(d) where only the states localized on one edge of the ribbon are shown.

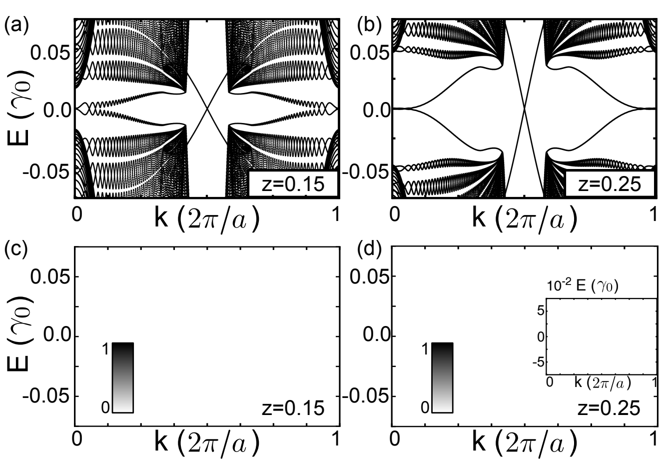

FIG. S5. (a) and (b): Full quasi-energy band structure for two laser intensities, $z = 0.15$ (a) and $z = 0.25$ (b). (c) and (d) represent the same data but with a color scale showing the weight of the corresponding eigenstate on the $n = 0$ Floquet channel. White is for zero weight and black is for unit weigth. These results are for $\hbar\Omega = 1.5\gamma_0$ and zigzag terminated leads with $W = 99a$. The inset in (d) shows the weight of the states on sites up to $2.5a$ from one of the sample edges (summed over all replicas).

[1] T. Oka and H. Aoki, Phys. Rev. B **79**, 081406 (2009).
[2] H. L. Calvo, H. M. Pastawski, S. Roche, and L. E. F. Foa Torres, Appl. Phys. Lett. **98**, 232103 (2011).
[3] M. Moskalets and M. Büttiker, Phys. Rev. B **66**, 205320 (2002).
[4] S. Kohler, J. Lehmann, and P. Hänggi, Physics Reports **406**, 379 (2005).
[5] L. E. F. Foa Torres, S. Roche, and J. C. Charlier, *Introduction to Graphene-Based Nanomaterials: From Electronic Structure to Quantum Transport* (Cambridge University Press, 2014).
[6] P. M. Perez-Piskunow, G. Usaj, C. A. Balseiro, and L. E. F. Foa Torres, Phys. Rev. B **89**, 121401(R) (2014).
[7] G. Usaj, P. M. Perez-Piskunow, L. E. F. Foa Torres, and C. A. Balseiro, Phys. Rev. B **90**, 115423 (2014).